



ISSN: 2319-5967

ISO 9001:2008 Certified

International Journal of Engineering Science and Innovative Technology (IJESIT)

Volume 6, Issue 2, March 2017

# Predictive Capability of the $k-\omega$ SST and Spalart-Allmarus Turbulence Models for a Double-Element Front Wing in Ground Effect-A CFD Analysis

Wael Mokhtar, Shardul Kachare

*Abstract—Nowa days, aerodynamics plays a significant role in determining a race win in an open wheel racecar championship such as Formula 1 and IndyCar. Since the front wing is the first part which meets the airflow and it determines the flow over the entire vehicle, a lot of research has been conducted to improve its aerodynamic efficiency. A modern racecar front wing can generate about 30% of the total downforce. The present study investigates the ability of Spalart-Allmarus and the standard  $k-\omega$  Shear Stress Transport (SST) turbulence models to predict the flow over a double-element front wing in ground effect. Also, the ability of unstructured polyhedral and trimmer meshing models was investigated. A three-dimensional computational study was conducted using Reynolds Averaged Navier Stokes (RANS) equations for a highly cambered double element single slotted modified NASA GA(W) profile of type LS (1)-0413 profile front wing with a total chord length of 380mm in ground effect. It was observed that the RANS model was correctly able to predict the flow over the double element front wing in ground effect. Both the turbulence models were able to predict the flow over the front wing in decreasing ground clearance and indicated the regions of force enhancement and force reduction. However, it was observed that for low ground clearances, the standard  $k-\omega$  SST turbulence model is best suited as it was able to predict the flow more accurately. Moreover, the results indicated, the use of unstructured polyhedral mesh model for meshing of wing is more effective.*

*Index Terms—CFD, Double-element, Front Wing, Ground effect, Turbulence models.*

## I. INTRODUCTION

Even though the concept of making use of inverted airfoils as racecar wings to generate downforce was first implemented in 1920's, it was not until 1965 that Formula 1 implemented them. The first rear wings appeared in 1965 on Lotus 49B and two weeks after that the first front wings appeared [1]. Since then, aerodynamics has been used as an effective tool to generate downforce and achieve higher cornering speeds by racecars in open wheel racecar series like Formula 1 and IndyCar. A conventional airfoil used in aircraft industry is designed to generate upward lift. Racecar wings are nothing but a conventional airfoil inverted generating a negative lift known as downforce, thus, providing more grip to go around corners at higher speeds [2].

Acknowledging the importance of aerodynamically efficient racecars, a lot of research has been conducted to improve the efficiency of racecar wings over the past three decades. Since a racecar wing is an inverted airfoil, it introduces some additional parameters such as ground effect, small aspect ratio and strong interaction between wing and other vehicle components, which has a significant effect on the aerodynamic forces generated [3]. The front wing in particular, has been a keen topic for research as it is the first part that comes into contact with the freestream airflow and it determines the flow over the vehicle. There exist several experimental and numerical studies explaining the aerodynamic characteristics of a typical front wing. To investigate the effect of varying ground clearance on both single and double element front wing, a series of experimental and numerical studies were conducted by Ranzenbach and Barlow [4], [5] and [6] using Reynolds Averaged Navier Stokes (RANS) equations. In these studies, a stationary ground clearance was used and the RANS equations were able to predict the flow over the front wing accurately with the help of two turbulence models. The  $k-\epsilon$  turbulence was used for majority of the study whereas, the one equation  $k-l$  turbulence model for the near wall viscous sublayer. It was observed that, for ground clearances of  $0.3c$  to  $0.1c$ , there exist a force enhancement region where downforce behaves as a function of ground clearance, i.e., downforce increases with decreasing ground clearance. Also, for lower ground clearances approximately less than  $0.1c$ , the downforce generated reduces also known as a force reduction region. The authors stated the reason was, the merging of ground plane and airfoil boundary layers. Mokhtar in his study [7] on S1223, E423, LNV109A and NACA9315 profiles, showed that the ground clearance



ISSN: 2319-5967

ISO 9001:2008 Certified

International Journal of Engineering Science and Innovative Technology (IJESIT)

Volume 6, Issue 2, March 2017

and angle of attack has significant impact in determining the downforce generated by a front wing. Mokhtar also studied the characteristics of NACA0012[8] concluding that downforce behaves as function of ground clearance. In addition, the effect of endplates on front wing was also studied on the S1223 profile by Mokhtar and Lanein another numerical study [9]. In another study by Mokhtar and Durrer [10] on S1223 profile, it was stated that the force reduction is a phenomenon which occurs as a result of merging of boundary layers.

Furthermore, to get more realistic results, experimental studies were conducted by Zhang and Zerihan[11] [12] on both a single and double element front wing in ground effect of the Tryrelle 026 Formula 1 racecar using a moving ground simulation. It was stated that, the separation of boundary layers at the trailing edge is the reason for reduction in downforce at very low ground clearances. Zhang and Mahon conducted two-dimensional computational studies [13] [14] on a single and double-element front wing used in the studies [11] [12] to investigate the predictive capabilities of RANS equations using six different turbulence models with a moving ground simulation. It was found that the RANS equations were successfully able to generate credible results. Furthermore, for lower ground clearance,  $k-\omega$  SST model gave the best results and the reduction in downforce was correctly predicted by it. However, the Realizable  $k-\epsilon$  model failed to predict flow at these lower ground clearances. In another similar two-dimensional numerical study for a single element front wing in ground effect by Genua [15] the predictive capability of the one equation Spalart-Allmarus, Realizable  $k-\epsilon$  and the standard  $k-\omega$  SST turbulence models was investigated. It was found that, the one equation Spalart-Allmarus turbulence model proved to be the best for predicting the flow and aerodynamic forces generated.

## II. PRESENT STUDY

In the present study, a three-dimensional computational analysis is performed for a freestream velocity of 30m/s which represents the usual cornering speeds in Formula 1. The wing model is studied for three different ground clearances of  $0.224c$ ,  $0.09c$  and  $0.05c$  and the predictive capability of two turbulence model is investigated.

### A. Wing Model

For the present study, the airfoil used is a highly cambered multi-element front wing consisting of two elements in a single slotted flap configuration. The main element is a modified NASA GA(W) profile of type LS (1)-0413 profile possessing a finite trailing edge of 1.56mm. The flap profile represents a typical profile used within motorsport and possesses a finite trailing edge of 0.95mm. Both the elements are inverted to have suction surfaces closest to the ground. The main element ( $c_m$ ) and flap ( $c_f$ ) has a chord of 223.4mm and 165.7mm respectively. For ease of calculations, the total chord of 380mm is used for all calculations. Furthermore, a constant total angle of attack ( $\alpha_o$ ) of zero degrees is used for the study with a low flap angle configuration. Zerihan and Zhang conducted the optimization of flap location for the said front wing [12] and came up with optimum values for flap gap ( $\delta_g$ ) and overlap ( $\delta_o$ ). These values are 9mm and 12mm for the overlap and gap respectively. In addition, the wing has a span of 1100mm and an aspect ratio of  $AR = 2.89$ . The ground clearance is taken as a ratio of vertical distance between the ground and lowermost point on the wing ( $H$ ) to its chord ( $c$ ) and is denoted as  $H/c$ . The described wing model is developed in SolidWorks 2016 and Figure 1 shows the schematic diagram of the wing model used in the present study.

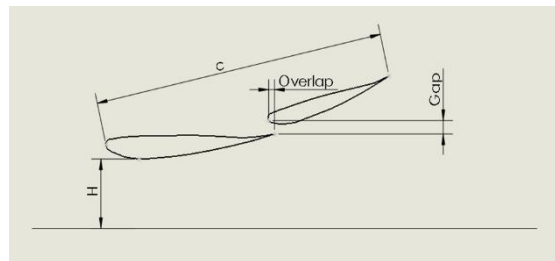


Fig 1: Schematic diagram of wing model.

### B. Numerical Model

For the present study, a three-dimensional computational analysis is conducted using a CFD package STAR CCM+, a finite volume method code for structured and unstructured meshes developed by CD-Adapco Inc. A freestream velocity of 30m/s corresponding to the Reynolds number of  $7.86 \times 10^5$  based on chord length is selected as it represents the cornering speed in Formula 1. STAR CCM+ solves the Reynolds Averaged Navier Stokes (RANS) equations to model the fluid flow. These equations are based off the fundamental physics



ISSN: 2319-5967

ISO 9001:2008 Certified

International Journal of Engineering Science and Innovative Technology (IJESIT)

Volume 6, Issue 2, March 2017

equations for conservation of mass, momentum, and energy. In the present study, a segregated flow model is used to solve for the three-dimensional RANS equations. The equations below show the three-dimensional RANS equations for an incompressible flow.

$$\rho \left( \frac{\partial u}{\partial t} + u \frac{\partial u}{\partial x} + v \frac{\partial u}{\partial y} + w \frac{\partial u}{\partial z} \right) = -\frac{\partial p}{\partial x} + \mu \left( \frac{\partial^2 u}{\partial x^2} + \frac{\partial^2 u}{\partial y^2} + \frac{\partial^2 u}{\partial z^2} \right) + \rho g_x \quad (1)$$

$$\rho \left( \frac{\partial v}{\partial t} + u \frac{\partial v}{\partial x} + v \frac{\partial v}{\partial y} + w \frac{\partial v}{\partial z} \right) = -\frac{\partial p}{\partial y} + \mu \left( \frac{\partial^2 v}{\partial x^2} + \frac{\partial^2 v}{\partial y^2} + \frac{\partial^2 v}{\partial z^2} \right) + \rho g_y \quad (2)$$

$$\rho \left( \frac{\partial w}{\partial t} + u \frac{\partial w}{\partial x} + v \frac{\partial w}{\partial y} + w \frac{\partial w}{\partial z} \right) = -\frac{\partial p}{\partial z} + \mu \left( \frac{\partial^2 w}{\partial x^2} + \frac{\partial^2 w}{\partial y^2} + \frac{\partial^2 w}{\partial z^2} \right) + \rho g_z \quad (3)$$

The computational domain consists of the wing model placed in a far field of length 2000mm, width 5500mm and height of 1750mm. The wing is placed about 500mm downstream in the far field. For boundary conditions, the wing and the ground is defined as a wall boundary with no-slip condition. The wing is applied with a no slip condition where  $U=V=0$  exists. Furthermore, since a moving ground simulation is used, the ground moves with a relative velocity of 30m/s in x-direction to the air. The figure 2 shows the three-dimensional computational domain used in the study along with the wing model.

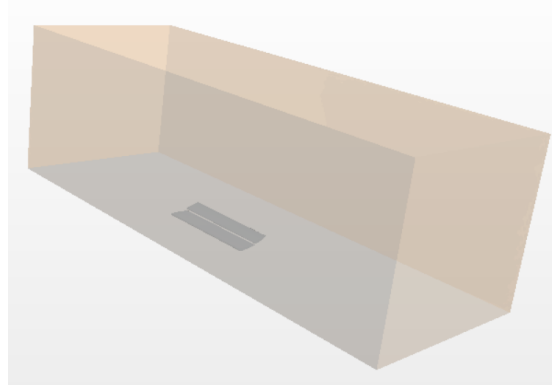


Fig 2: Computational domain used along with the wing model.

In the present study, the applicability of two meshing models for a three-dimensional wing model is investigated. The two meshing models used are, an unstructured polyhedral and a structured trimmer mesh models. In addition, to effectively determine the applicability of both the models, the reference values for both models are kept similar.

### C. Turbulence Model

The predictive capability of two turbulence models for a flow over a front wing in ground effect is investigated in this study. The two turbulence models used are the one equation Spalart-Allmarus and the standard  $k-\omega$  Shear Stress Transport (SST) turbulence models. The one equation Spalart-Allmarus turbulence model as the name suggests is a one equation turbulence model developed by P. R. Spalart and S. R. Allmarus [16]. This model uses one equation to calculate the eddy viscosity and hence is numerically efficient. It is usually used for simple geometries such as airfoils. However, it can be used for predicting separated flows. On the other hand, the standard  $k-\omega$  Shear Stress Transport (SST) model makes use of two equations to solve for the unknowns [17]. It's an integration of the standard  $k-\epsilon$  and  $k-\omega$  turbulence models. In simple terms, the standard  $k-\omega$  SST model is used between these two model to overcome their shortcomings. For instance, to predict flow near wall and for completely developed flow far from wall, it makes use of  $k-\epsilon$  model. Whereas, to predict flow for outer boundary layers and in regions of separation, it makes use of  $k-\omega$  model. Thus, the standard  $k-\omega$  SST model is highly efficient and is widely used for most of the studies. Furthermore, a turbulent viscosity ratio of 10 is used for the present study.

## III. RESULTS AND DISCUSSION

### A. Meshing

The applicability of an unstructured polyhedral and a structured trimmer mesh meshing models is investigated in this study. For the similar reference value for each model and at a ground clearance of  $0.224c$ , a volume mesh of the three-dimensional wing model is generated compared. The figure 3 shows a cross sectional view of the volume mesh generated at mid-plane of the wing.

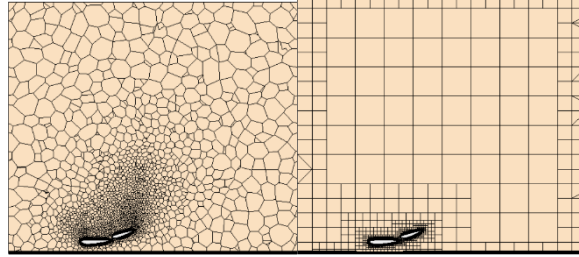


Fig 3: Volume mesh of at mid-plane using polyhedral (left) & trimmer (right) mesh model.

It can be observed from the figure 3 that, for same configuration, the unstructured polyhedral mesh model was able to capture a more refined mesh with a comparatively steady growth rate. The cells along the far end of far field merge in a smoother manner in polyhedral model thus giving a more refined mesh. The uniform growth rate for the three-dimensional volume mesh can be clearly seen in the figure 4 which shows the volume mesh of wing model using both models.



Fig 4: : Mesh of a wing model using polyhedral (left) and trimmer (right) mesh model.

Thus, for further analysis the unstructured polyhedral mesh is used for meshing and depending on the ride height, around 500,000 to 2 million cells are generated for volume mesh. Also, a refinement block is created to capture to area between the lower suction surface of wing and the ground. The final mesh for a ride height of  $0.224c$  with the use of a refinement block is shown in figure 5.

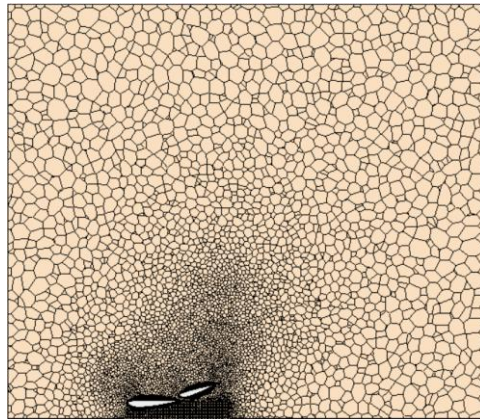


Fig 5: Final mesh of mid-plane section with the refinement block

## B. Turbulence

In the present study, a three-dimensional computational analysis is conducted to determine the predictive capabilities of the one equation Spalart-Allmarus and the standard  $k-\omega$  Shear Stress Transport (SST) turbulence models for a double-element front wing in ground effect for three different ground clearances. Three different ground clearances of  $0.224c$ ,  $0.09c$  and  $0.05c$  are studied for a moving ground simulation. The results for the aerodynamic forces generated are compared with the existing experimental study conducted in [12].

### 1. Medium ground clearance of $0.224c$

For the given ground clearance both the models were able to predict the flow over the double-element front wing correctly. The highly-cambered double-element single slotted front wing generates downforce with the help of

Bernoulli's principle. The air flowing on the lower surface of the wing is forced downwards which compresses it against the air below it and the ground. However, the air flowing over the upper surface is expanded. Due to the compression, the air flowing on lower surface flows at a higher velocity whereas, the air on upper surface flows at lower velocity due to expansion. Now due to Bernoulli's principle, the air flowing at higher velocity experiences lower pressure than the air flowing on lower region. This pressure difference between the upper and lower surfaces creates a force in downward direction, which is known as downforce.

By analyzing the velocity and pressure distribution plots both the turbulence models were able to predict this phenomenon accurately at ground clearance of  $0.224c$ . The figures show the velocity and pressure distribution plots using the one equation Spalart-Allmarus and the standard  $k-\omega$  Shear Stress Transport (SST) turbulence models.

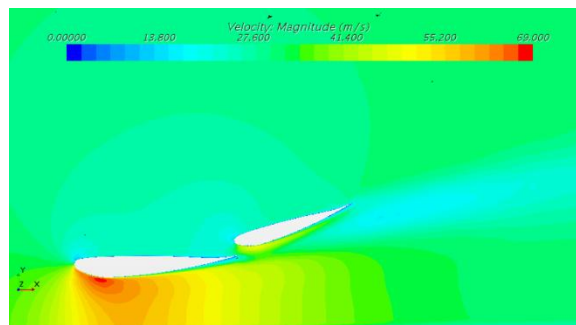


Fig 6: Velocity contour for mid-span plane using  $k-\omega$  SST

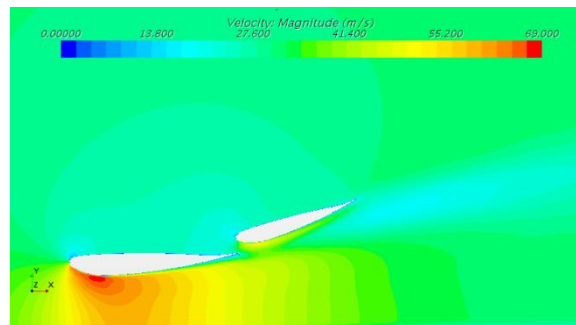


Fig 7: Velocity contour for mid-span plane using Spalart-Allmarus

From the velocity vector distribution plots, the accelerated flow below the lower surface can be clearly seen. The air flows at an accelerated speed of about 100% than the freestream flow.

Furthermore, both the turbulence models were able to show the formation of separation of boundary layer at the trailing edge. The pressure distribution plot for the two models show this phenomenon clearly in figures 8 and 9.

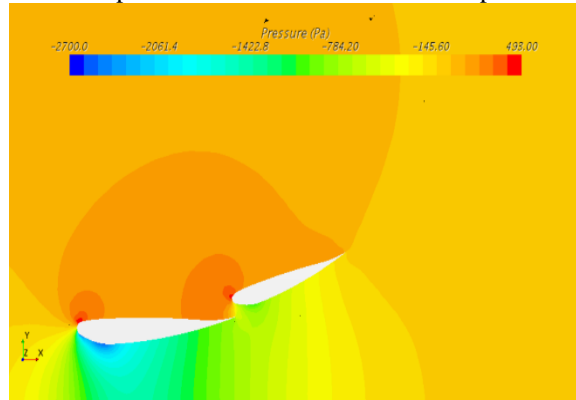
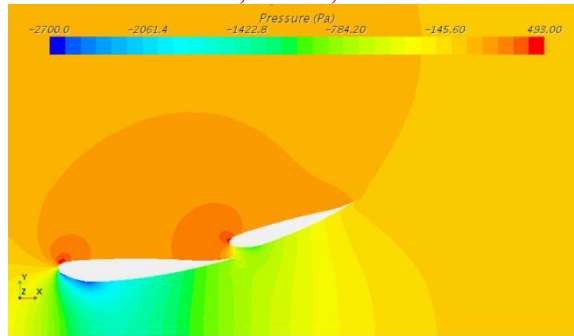


Fig 8: Pressure contour for mid-span plane using  $k-\omega$  SST



**Fig 9: Pressure contour for mid-span plane using Spalart-Allmarus**

In order to measure the negative lift or downforce generated by the wing at this ground clearance for both models, the lift coefficient ( $C_L$ ) is calculated and compared with an existing study [11]. Both the turbulence models accurately predicted the value of lift coefficient at the ground clearance of  $0.224c$ .

**2. Low ground clearance of  $0.09c$**

As the ground clearance is lowered, the air flow between the wing and ground is accelerated further thus, generating more downforce. By lowering the ground clearance from  $0.224c$  to  $0.09c$ , the velocity of air on the lower surface of wing increased by 18.8% causing a reduction in pressure. As a result of this, the lift coefficient is increased by about 36%. Hence, indicating that the downforce indeed behaves as a function of ground clearance. The air below the lower surface gets accelerated by about 172% than the freestream air. The velocity distribution plots clearly show the further accelerated air in figures 10 and 11 using both turbulence models. Also, by observing the pressure distribution contours in figures 12 and 13, the separation of boundary layers at the trailing edge appears to increase as the ground clearance is reduced.

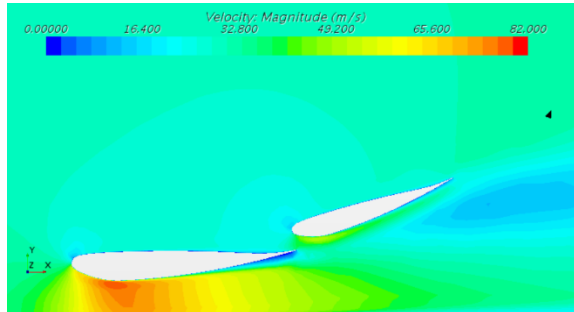


**Fig 10: Velocity contour for mid-span plane using k- $\omega$  SST**

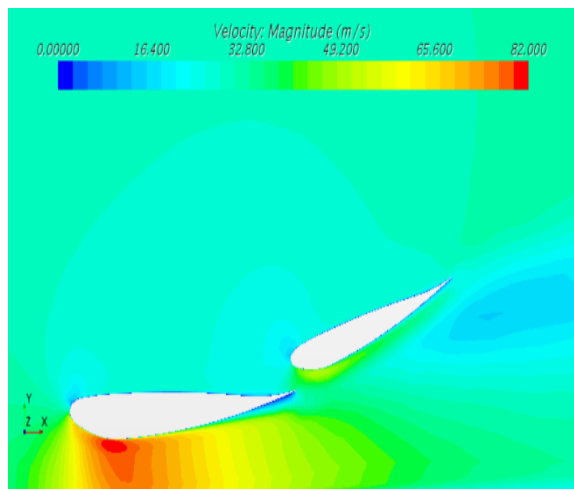


**Fig 11: Velocity contour for mid-span plane using Spalart-Allmarus**

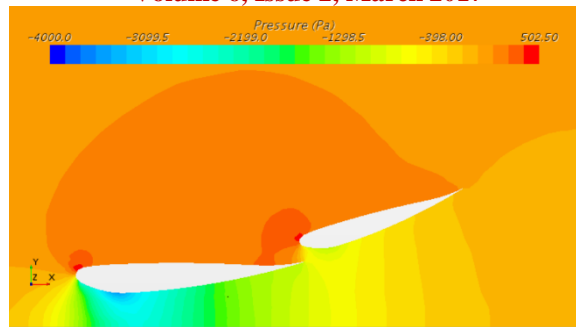


Fig 12: Pressure contour for mid-span plane using  $k-\omega$  SST

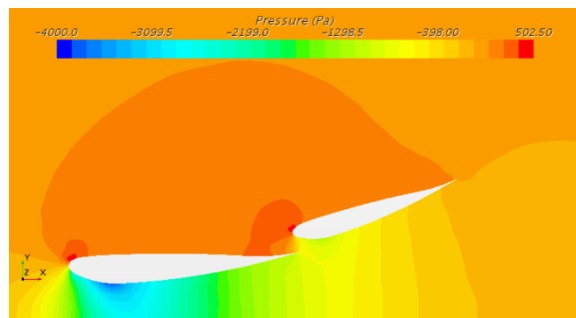


Fig 13: Pressure contour for mid-span plane using Spalart-Allmarus

By observing the velocity and pressure contours for both the turbulence models, it is found that the one equation Spalart-Allmarus model shows a higher accelerated flow than the standard  $k-\omega$  SST model thus, also relating to a lower suction pressure. Furthermore, by comparing the values for lift coefficient for the both the turbulence models, it appears that the standard  $k-\omega$  Shear Stress Transport (SST) turbulence model is more accurate than the one equation Spalart-Allmarus. The value of lift coefficient using standard  $k-\omega$  SST turbulence model is more accurate with 5.6% error. Whereas, the one equation Spalart-Allmarus predicts the lift coefficient with a 11.3% error.

### 3. Very low ground clearance of $0.05c$

When the ground clearance is reduced further, the downforce generated by the wing is reduced. Thus, indicating that for very low ground clearances, a downforce reduction occurs due to the separation of boundary layers at the trailing edge for very low ground clearances and there exists a maximum lift coefficient for a particular ground clearance. The separation of boundary layer at the trailing edge occurs due to the boundary layer not being able to withstand the adverse pressure gradient associated with highly accelerated flow at small ride heights. The separation of boundary layer at the trailing edge can be clearly seen by observing the velocity and pressure contours in figures 14 to 17.

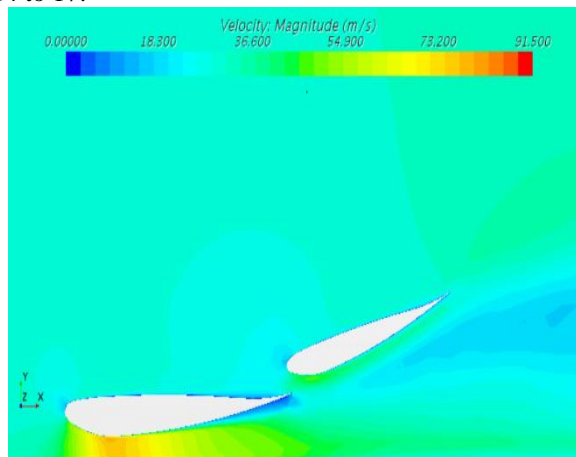


Fig 14: Velocity contour for mid-span plane using  $k-\omega$  SST

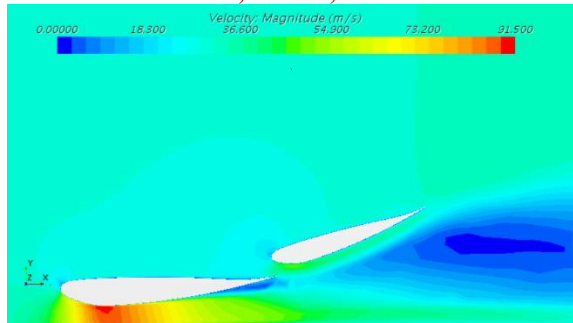


Fig 15: Velocity contour for mid-span plane using Spalart-Allmarus

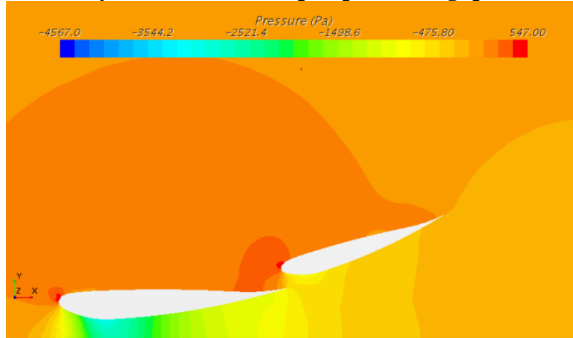


Fig 16: Pressure contour for mid-span plane using  $k-\omega$  SST

Furthermore, for this very low ground clearance, the standard  $k-\omega$  SST turbulence model is able to predict the lift coefficient more accurately than the one equation Spalart-Allmarus. The value of lift coefficient at  $0.05c$  for standard  $k-\omega$  SST turbulence is more accurate with a 5.28% error when compared to the 20.94% error for the one equation Spalart-Allmarus. The accuracy of both the turbulence models to predict the flow is observed by the graph of lift coefficient ( $C_L$ ) against the ground clearance in figure 17 below.

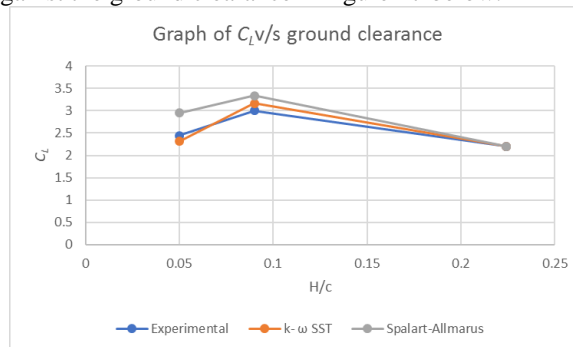


Fig 17: Graph of  $C_L$  v/s  $H/c$

#### IV. CONCLUSION

A three-dimensional computational analysis to determine the predictive capability of the one equation Spalart-Allmarus and the standard  $k-\omega$  Shear Stress Transport (SST) turbulence models for a double-element front wing in ground effect was successfully performed and following conclusions can be made:

- The Reynolds Averaged Navier Stokes (RANS) equations are successfully able to predict the flow over a double-element front wing computationally.
- The unstructured polyhedral meshing model is best suited for meshing the wing model.
- For medium ground clearance of  $0.224c$ , both the turbulence models are able to accurately predict the flow.
- For low ground clearance of  $0.09c$  and very low ground clearance of  $0.05c$ , the standard  $k-\omega$  Shear Stress Transport (SST) turbulence model is best suited as its able to predict the flow more accurately.





ISSN: 2319-5967

ISO 9001:2008 Certified

International Journal of Engineering Science and Innovative Technology (IJESIT)

Volume 6, Issue 2, March 2017

REFERENCES

- [1] Seljak, G. (2008). Race Car Aerodynamics. Ljubljana.
- [2] Guarro, M. D. (2010). Wing Efficiency of Race Cars. Santa Cruz: University of California.
- [3] Katz, J. (2006). Aerodynamics of Race Cars. Annual Review of Fluid Mechanics, (pp. 27-63).
- [4] Ranzenbach, R., & Barlow, J. B. (1994). Two-Dimensional Airfoil in Ground Effect, An Experimental and Computational Study. Motorsport Engineering Conference. 1, pp. 241-249. SAE International.
- [5] Ranzanbach, R., & Barlow, J. B. (1997). Cambered Airfoil in Ground Effect. AIAA.
- [6] Ranzenbach, R., Barlow, J. B., & Diaz, R. H. (1997). Mult-Element Airfoil in Ground Effect-An Experimental and Computational Study. AIAA.
- [7] Mokhtar, W. A. (2005). A Numerical Study of High-Lift Single Element Airfoils with Ground Effect for Racing Cars. Norfolk: SAE International.
- [8] Mokhtar, W. A. (2008). Aerodynamics of High-Lift Wings with Ground Effect for Racecars. Sault Ste Marie: SAE International.
- [9] Mokhtar, W., & Lane, J. (2008). Racecar Front Wing Aerodynamics. SAE International.
- [10] Mokhtar, W., & Durrer, S. (2016). A CFD Analysis of a Race Car Front Wing in Ground Effect. 2016 ASME North Central Section Conference.
- [11] Zerihan, J., & Zhang, X. (2000). Aerodynamics of a Single Element Wing in Ground Effect. Journal of Aircraft, 1058-1064.
- [12] Zhang, X., & Zerihan, J. (2003). Aerodynamics of a Double-Element Wing in Ground Effect. AIAA, 1007-1016.
- [13] Mahon, S., & Zhang, X. (2004). Computational Analysis of Pressure and Wake Characteristics of an Aerofoil in Ground Effect. Journal of Fluids Engineering.
- [14] Mahon, S., & Zhang, X. (2006). Computational Analysis of an Inverted Double-Element Wing in Ground Effect. Southampton: University of Southampton.
- [15] Genua, E. (2009). A CFD Investigation into Ground Effect Aerodynamics. Netherlands: Delft University of Technology.
- [16] Spalart, P., & Allmarus, S. (1992). The One Equation Turbulence Model for Aerodynamic Flow. AIAA 30th Aerospace Sciences Meeting and Exhibition. Reno, Nevada.
- [17] Menter, F. R. (1993). Zonal Two Equation k-  $\epsilon$  Turbulence Models for Aerodynamic Flows. 24th Fluid Dynamics Conference. Orlando, Florida: AIAA.